ACS Catalysis

Research Article

pubs.acs.org/acscatalysis

Double-Supported Silica-Metal–Organic Framework Palladium Nanocatalyst for the Aerobic Oxidation of Alcohols under Batch and Continuous Flow Regimes

Vlad Pascanu,[†,‡,#] Antonio Bermejo Gómez,[†,‡,#] Carles Ayats,[∥] Ana Eva Platero-Prats,[‡,§] Fabian Carson,[‡,§] Jie Su,[‡,§] Qingxia Yao,[‡,§] Miquel À. Pericàs,[∥,⊥] Xiaodong Zou,*[,‡,§] and Belén Martín-Matute*[,†,‡]

[†]Department of Organic Chemistry, [‡]Berzelii Center EXSELENT on Porous Materials, and [§]Department of Materials and Environmental Chemistry, Stockholm University, Stockholm SE-10691, Sweden

[∥]Institute of Chemical Research of Catalonia, E-43007 Tarragona, Spain

[⊥]Department of Organic Chemistry, University of Barcelona, E-08028 Barcelona, Spain

Supporting Information

ABSTRACT: Stable and easily synthesized metal–organic framework MIL-88B-NH_2 represents an attractive support for catalysts employed in oxidation reactions, which are typically performed under relatively harsh conditions. However, MIL-88B-NH_2, the thermodynamic polymorph of the more popular MIL-101-NH_2, has been rarely employed in catalytic applications because of a difficult impregnation process caused by the flexible nature of the framework. We report herein a new catalyst denoted Pd@MIL-88B-NH_2 (8 wt % Pd), the first example of metallic nanoparticles successfully impregnated in the pores of MIL-88B-NH_2. Furthermore, by enclosing the MOF crystals in a tailored protective coating of SiO_2 nanoparticles, an even more enduring material was developed and applied to the aerobic oxidation of benzylic alcohols. This doubly supported catalyst Pd@MIL-88B-NH_2@nano-SiO_2 displayed high activity and excellent performance in terms of endurance and leaching control. Under batch conditions, a very convenient and efficient recycling protocol is illustrated, using a "teabag" approach. Under continuous flow, the catalyst was capable of withstanding 7 days of continuous operation at 110 °C without deactivation. During this time, no leaching of metallic species was observed, and the material maintained its structural integrity.

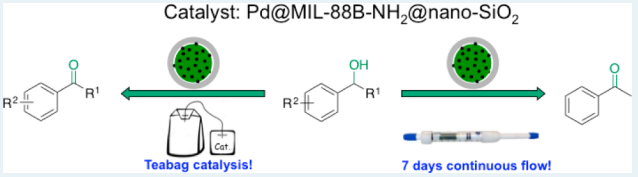

KEYWORDS: *palladium nanoparticles, MIL-88B-NH_2, aerobic oxidation, teabag catalysis, flow chemistry*

INTRODUCTION

The aerobic oxidation of alcohols is an important industrial process. Sustained interest in the field is partially driven by the prospect of applying aerobic oxidation to biomass conversion, which is an abundant source of alcohols.[1] Recent advances in the area aim to use mild conditions and replace hazardous reagents with air as the oxidant.[2] Supported heterogeneous oxidation catalysts[3] have also received widespread attention because they can be recovered and recycled,[4] and palladium is often the transition metal chosen to perform the oxidation reaction.[5] For example, Pd@ARP (amphiphilic resin)[6] was used for the aerobic oxidation of secondary alcohols in water, and Pd@SBA-15 (SBA, functionalized Santa Barbara amorphous silica material)[7] was used to oxidize benzylic alcohols at temperatures as low as 80 °C. Hutchings and co-workers reported that Au–Pd bimetallic core–shell nanoparticles supported on TiO_2 could selectively oxidize benzylic and allylic alcohols with exceptional turnover frequencies (269 000 h^{-1}) under neat conditions at 100–160 °C.[8]

Metal–organic frameworks (MOFs) are porous crystalline materials assembled from metallic ions or clusters and organic multitopical linkers.[9] MOFs have gained popularity as supports in heterogeneous catalysis[10,11] because of their high surface areas and large pore volumes, which can accommodate the active catalytic sites. Another advantage is the possibility to modify MOFs postsynthetically in order to tune the properties of the framework.[12] Metallic nanoparticles can be stabilized in the pores of MOFs through both mechanical and charge-transfer interactions.[13] Through these mechanisms, highly active, small nanoparticles with a narrow size distribution can be generated, and their leaching can be avoided, facilitating the recycling of the catalyst. On the basis of these properties, combining the benefits of MOFs and flow chemistry can be regarded as a natural direction for progress in the field, and we recently reported the first example of metallic nanoparticles supported on MOFs for flow processes.[11d]

Among the first MOF-supported catalysts employed for the oxidation of alcohols, Li and co-workers developed a Pd catalyst supported on MIL-101-NH_2.[14] This system displayed good efficiency if molecular oxygen was bubbled through the reaction

Received: October 14, 2014
Revised: November 24, 2014
Published: November 26, 2014

mixture at a sufficiently high rate. The authors also suggest an important contribution from the acid sites in the framework for the outcome of the reaction. More recently, a modified version of UiO-66 was also shown to tolerate a very wide scope of substrates and to be recyclable in the presence of sacrificial oxidants (e.g., TBHP and H_2O_2).[15] Around the same time, it was shown that TiO_2 nanoparticles incorporated in the mesoporous HKUST-1 were capable of performing a photocatalytic oxidation of alcohols in moderate yields under sunlight irradiation.[16] However, it is well known that many MOFs suffer from poor mechanical strength compared to denser supports, such as ceramics.[17] On the basis of this limitation, we envisioned that coating the MOF with a protective layer could improve its stability and reusability for catalytic processes. An interesting solution consists of surrounding the catalyst with SiO_2 nanoparticles that contain mesopores between the particles, which were recently shown to improve the diffusion into the MOF.[18] In this way, the mechanical properties of the MOF are improved while also allowing reactants to reach the active sites.

Herein we report the development of a new palladium nanocatalyst protected by an innovative double-layered MOF@silica support. For the first time, the immobilization of metallic nanoparticles could be achieved in the flexible functionalized MIL-88B-NH_2 framework. This long-elusive goal was accomplished after investigating the manner in which the material responds to the polarity of its surrounding environment by alternating its open/close conformations. MIL-88B-NH_2 is the denser thermodynamic polymorph of the notorious MIL-101-NH_2, and thus the proposed catalyst is expected to withstand much harsher reaction conditions than previously reported Pd@MIL-101-type catalysts.[14,19] A good dispersion of the Pd nanoparticles is achieved in MOFs containing nitrogen functional groups in the organic linkers. These coordinating groups also contribute to reduce the metal leaching during catalysis.[20] Importantly, the functionalized MIL-88B-NH_2 MOF could be more conveniently synthesized directly from 2-aminoterephthalic acid, thereby avoiding wasteful postsynthetic modification procedures required for its MIL-101 analog.[21] The MOF was subsequently enclosed by SiO_2 nanoparticles to produce a more resistant material (Scheme 1) labeled Pd@MIL-88B-NH_2@nano-SiO_2. This material was also more suitable for stabilizing small nanoparticles and preventing metallic leaching than simple Pd@SiO_2 catalysts.[5c] The catalytic activity of this novel material was evaluated in the oxidation of benzylic alcohols to their corresponding carbonyl compounds using only air as the oxidant, at ambient pressure without using any bubbling device. The benefits of this new support are also demonstrated by the outstanding properties of the catalyst under a continuous-flow regime. When packed in a microflow reactor, the material can endure more than 7 days of continuous operation without diminishing its efficiency. Metal leaching is minimized throughout the whole experiment, and high total turnover numbers are achieved. Therefore, this is a more durable catalyst than previously reported, synthesized in a more economical manner, fulfilling the main directives of green chemistry through catalysis: efficiency, sustainability, and recyclability.[22−25]

Scheme 1. Graphical Illustration of the Synthesis of Pd@MIL-88B-NH_2@nano-SiO_2

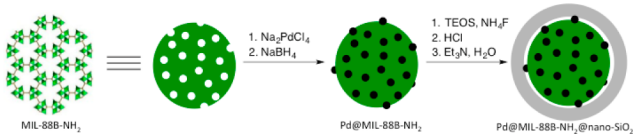

RESULTS AND DISCUSSION

Synthesis of Pd@MIL-88B-NH_2@nano-SiO_2. MIL-88B-NH_2 was synthesized under solvothermal conditions and activated according to an adapted procedure from Lin and co-workers.[26] The crystallinity of the MOF was confirmed by X-ray powder diffraction (XRPD) and is shown in Figure 1a.

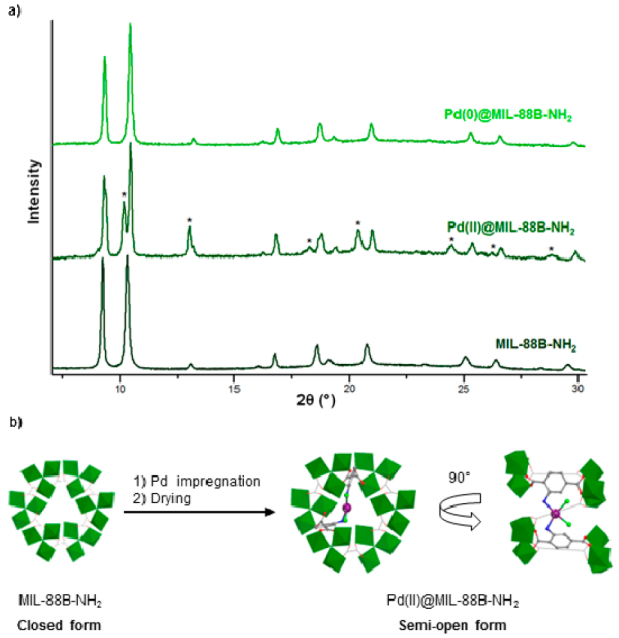

Figure 1. (a) XRPD patterns of MIL-88B-NH_2, Pd(II)@MIL-88B-NH_2, and Pd(0)@MIL-88B-NH_2 and (b) schematic polyhedral representation of Pd(II) impregnation in MIL-88B-NH_2. The purple ball represents Pd. The blue and light green balls represent nitrogen and chloride, respectively. The Pd(II) species lead to MIL-88B-NH_2 adopting a semi-open form, highlighted in the XRPD patterns by asterisks (*).

The impregnation of this MOF with palladium can be challenging because of the flexible nature of the framework. A screening experiment using solvents with different polarities confirmed that the impregnation is more efficient with polar solvents and the best results were obtained in MeOH (ESI, Table S1).[27] The structure of MIL-88B expands in MeOH,[28] which facilitates the introduction of Pd(II) complexes into the MOF pores. Higher loadings of palladium were achieved with Na_2PdCl_4 when compared to $PdCl_2(CH_3CN)_2$, and after 72 h, loadings of between 7.15 and 8.60 wt % were achieved, as determined by ICP-OES analysis. This corresponds to a Pd/Cr ratio of 1:4 and ∼26% functionalization of the amino-terephthalate linkers.[29] $NaBH_4$ was then used to reduce Pd(II) and form palladium nanoparticles in the MOF [Pd(0)@MIL-88B-NH_2]. The XRPD pattern matched that of MIL-88B-NH_2, confirming the integrity of the framework upon functionalization (Figure 1a).[30]

Pd *K*-edge extended X-ray absorption fine structure (EXAFS) spectroscopy was performed on Pd(II)@MIL-88B-NH_2(Cr) to determine the coordination environment of

dx.doi.org/10.1021/cs501573c | ACS Catal. 2015, 5, 472−479

palladium (Figure 2a). The data were best fit using a *cis* square-planar geometry at the Pd(II) center, with the coordination

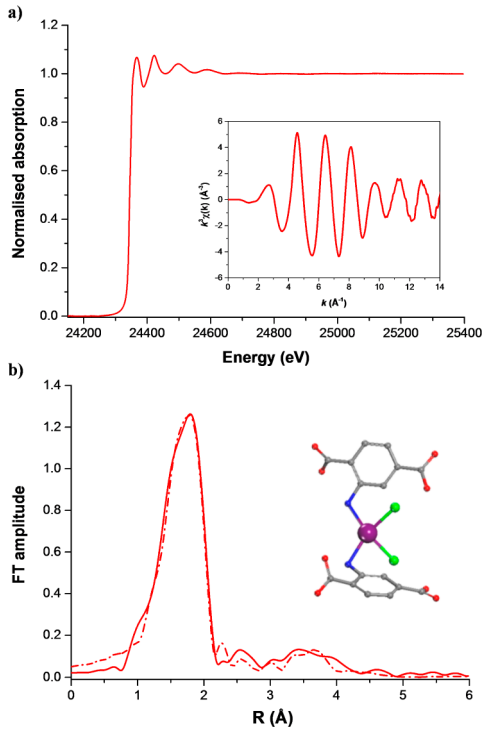

Figure 2. (a) Pd *K*-edge XAFS spectra for Pd(II)@MIL-88B-NH_2 and *k*-weighted XAFS, $\chi(k)k^3$ (detail). (b) Experimental (solid line) and fitted (dashed line) FT[$\chi(k)k^3$] functions (bottom) with $\Delta k \approx 2-14$ $Å^{-1}$. The palladium coordination environment was used to fit the EXAFS data (hydrogen atoms omitted for clarity). The purple ball represents palladium. The blue and light-green balls represent nitrogen and chloride, respectively.

environment comprising chloride anions and two amino groups (Figures 1b and 2b). The *cis* conformation appears to be more likely than the *trans* (ESI, Section S2), which agrees with palladium(II) complexes located in the pores of the MOFs' closed form (Figure 2). The data fitting indicated Pd bonds to two N atoms at 2.06(1) Å and two Cl atoms at 2.307(5) Å. These distances are in agreement with the crystallographic data of reported [Pd(II)$(ArNH_2)_2Cl_2$] complexes.[31] The nearest-neighbor carbon atom from the phenyl ring was determined at a distance of 3.38(5) Å, which is consistent with a semi-open form of this MOF (3.052 Å crystallographic value for the closed form).[32]

To further study the functionalization of MIL-88B-NH_2 with palladium complexes, we performed N_2 sorption experiments and LeBail refinements of the XRPD patterns (ESI, Figure S3). Pd(II)@MIL-88B-NH_2 contains two forms of MIL-88B: a closed form and a semi-open form in a ratio of ~70:30 (V = 1976(1) and 2099(1) $Å^3$, respectively, see Table S4). We attribute the presence of this semi-open form to Pd(II) attached to the amino groups in the MOF, which agrees with the results from EXAFS and ICP-OES (Figure 2). The underlying net of MIL-88B is acs-a,[33] which consists of packing six-membered rings in a chair conformation. MIL-88B is flexible, and palladium incorporation into the MOF changes the degree of pore opening. In addition, the BET surface area increases from 7 to 30 m^2/g after palladium impregnation, which implies that the MOF is partially locked in a semi-open form (ESI, Section S4).[30]

The reduction of Pd(II), following a procedure similar to that described for Pd(0)@MIL-101-NH_2,[18] afforded Pd(0)@MIL-88B-NH_2. A second layer of protection was achieved by coating the Pd(0)@MIL-88B-NH_2 crystals with nanosized SiO_2 particles (ESI, Section S1 for the detailed synthesis procedure). The material was washed with HCl (aq, pH 2) to remove residual TEOS, which can affect its catalytic performance. Traces of acid were neutralized with an aqueous solution of Et_3N. The integrity of the MOF framework was confirmed by XRPD, which contained a large background hump attributed to the silica (Figure 3a). This new material, denoted Pd@MIL-88B-NH_2@nano-SiO_2, contained 0.51 wt % Pd, as measured by ICP-OES analysis. It is noteworthy that a similar coating strategy applied to Pd@MIL-101-NH_2 led to the decomposition of the MOF and the formation of a completely amorphous material.

The Pd nanoparticles were evenly distributed in the MOF with an average particle size of 2 to 3 nm, as shown by transmission electron microscopy (TEM; ESI, Section S5). Furthermore, the presence of nanosized SiO_2 particles surrounding the Pd@MOF crystal surface is evident in Figure 3b. Some larger Pd agglomerates were visible on the MOF surface subsequent to silica coating (Figure 3b).

N_2 sorption experiments on Pd(0)@MIL-88B-NH_2 showed very low gas uptake, indicating that the closed form of the MOF is predominant. In contrast, the SiO_2-supported material displayed a type IV isotherm with significant N_2 uptake (Figure 3c).[34] This hysteresis is due to mesopores between the silica nanoparticles. The BET surface area and pore volume for Pd@MIL-88B-NH_2@nano-SiO_2 were calculated to be 603 ± 4 m^2/g and 1.82 cm^3/g, respectively (ESI, Section S4).

The TGA analyses of all materials showed a considerably improved thermal resistance (ca. 60 °C) of the doubly supported silica-MOF compared to that of the original Pd@MOF catalyst (ESI, Section S6).

CATALYTIC PROPERTIES

The properties of the new material were then investigated in terms of robustness and catalytic activity in the oxidation of secondary benzylic alcohols. Pd@MIL-88B-NH_2@nano-SiO_2 was demonstrated to be highly active and selective, using air as the oxidant in *p*-xylene at 150 °C, tolerating a wide variety of substitution patterns (Table 1). With typical substrates such as 1-phenylethanol (**1a**), 1-(4′-methylphenyl)ethanol (**1b**), 1-(4′-methoxyphenyl)ethanol (**1c**), and 1-phenylpropanol (**1d**), Pd@MIL-88B-NH_2@nano-SiO_2 (2 mol % Pd) returned the corresponding ketones (**2a**−**2d**) in excellent yields within reasonably short reaction times (Table 1, entries 1−4). Substrates containing cyclic motifs (Table 1, entry 6, **2f**) and bulky substituents on either side of the hydroxyl group (Table 1, entries 5 and 7−9, **2e** and **2g**−**2i**) were easily converted to the desired carbonyl compounds in reaction times ranging from 15 to 20 h and were isolated in excellent yields. More functionalized substrates, such as diol **1j** (Table 1, entry 10) and benzoin **1k** (Table 1, entry 11), were also transformed into the corresponding ketones (**2j**−**2k**) with no difficulties and in very good isolated yields. Although these last two substrates with electron-withdrawing groups afforded good results (**1j**−**1k**), other benzylic alcohols substituted with nitrogen-containing electron-withdrawing groups in the *para* position (**2l** and **2m**) could not be oxidized (Table 1, entries 12 and 13).

dx.doi.org/10.1021/cs501573c | ACS Catal. 2015, 5, 472−479

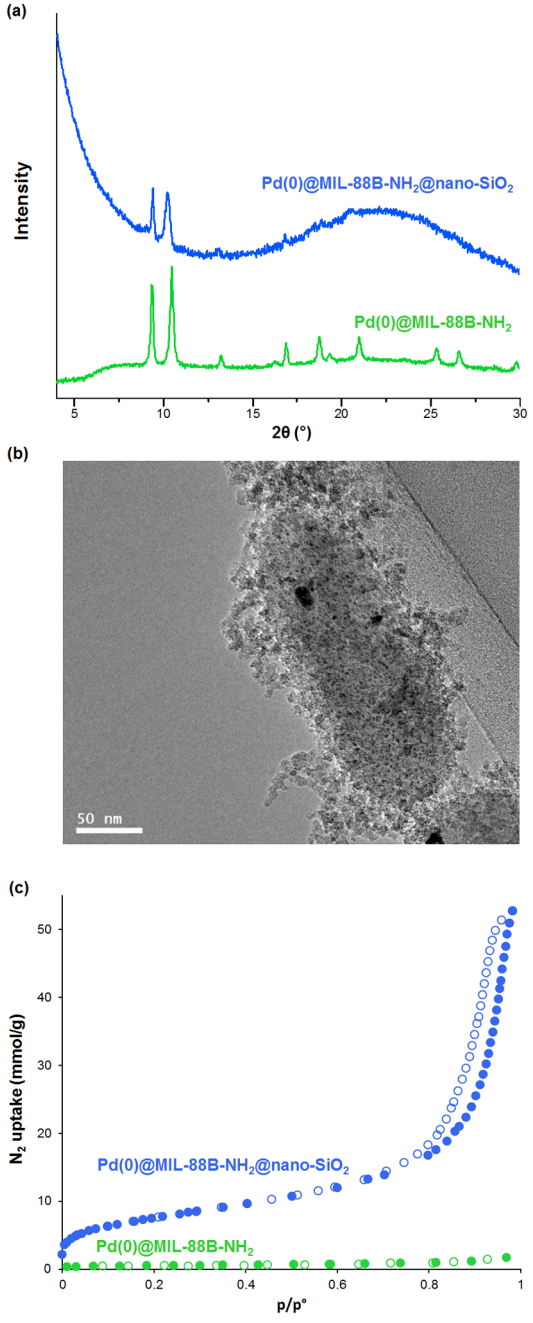

Figure 3. (a) XRPD patterns of Pd(0)@MIL-88B-NH_2 and Pd(0)@MIL-88B-NH_2@nano-SiO_2, (b) TEM micrograph of Pd(0)@MIL-88B-NH_2@nano-SiO_2, and (c) N_2 adsorption (filled symbols) and desorption (open symbols) isotherms of Pd(0)@MIL-88B-NH_2 and Pd(0)@MIL-88B-NH_2@nano-SiO_2.

However, alcohol **1n**, with a pyridyl substituent, afforded the product in good yield when 4 mol % Pd was used (Table 1, entry 14). Importantly, when 1-phenylethanol (**1a**) was reacted under neat conditions on a 10 mmol scale, the catalyst loading could be lowered to 0.04 mol % Pd and a full conversion could still be achieved within 12 h with complete selectivity toward the oxidation product (Table 1, entry 1). A blank silica material synthesized in a similar manner without the addition of Pd@MIL-88B-NH_2 was employed under the standard reaction conditions, but no conversion was observed. When the reaction

Table 1. Substrate Scope

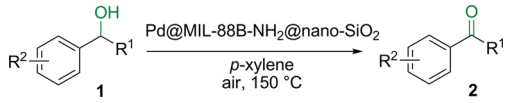

Entry	Product	Cat. loading [mol%]	Time [h]	Isolated Yield [%]
1	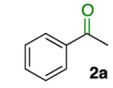 **2a**	2	10	98
		0.04[a]	12	97
2	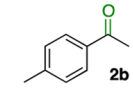 **2b**	2	15	90
3	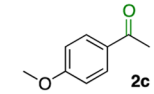 **2c**	2	12	63
4	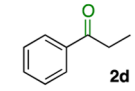 **2d**	2	15	97
5	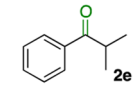 **2e**	2	15	95
6	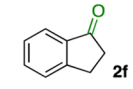 **2f**	2	12	94
7	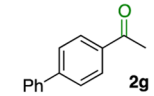 **2g**	2	20	97
8	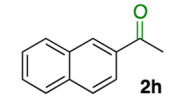 **2h**	2	15	87
9	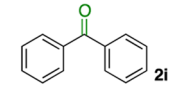 **2i**	2	15	97
10	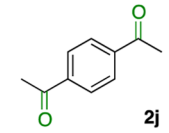 **2j**	2	15	68
11	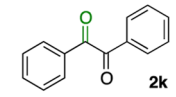 **2k**	5	10	85
12	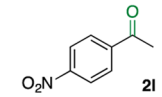 **2l**	2	68	n.d. (<10)[b]
		4	44	n.d. (<10)[b]
13	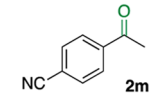 **2m**	2	68	n.d. (<10)[b]
		4	44	n.d. (<10)b
14	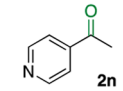 **2n**	2	44	n.d. (42)[b]
		4	24	71

[a]Reaction run under neat conditions, with no byproduct formation. [b]Yield estimated by ^{1}H NMR spectroscopy.

dx.doi.org/10.1021/cs501573c | ACS Catal. 2015, 5, 472−479

of **1a** was carried out without catalyst under an atmosphere of air at 150 °C for 20 h, **2a** was obtained in less than 5% yield.

RECYCLING EXPERIMENTS USING A CATALYTIC TEABAG

The beneficial effect of the innovative silica protective layer over the recyclability of the new material was demonstrated in a "teabag" experiment (Figure 4, Movie S1) showing that Pd@MIL-88B-NH_2@nano-SiO_2 is remarkably easy to handle and recycle. In contrast, the separation of the particles of Pd@MIL-88B-NH_2 (i.e., without silica) from the reaction mixtures is tedious, which is due to the small size of the silica-free particles and can be achieved only through centrifugation. The catalyst (200 mg of 0.51 Pd wt %, 1 mol %) in a teabag firmly tied with a Teflon wire was inserted into a solution of 1-phenylethanol (**1a**) in *p*-xylene. After 16 h at 150 °C, the catalyst was pulled out using the attached Teflon wire and subsequently immersed in a fresh reaction batch. This facile recycling process could be repeated four times to obtain very good yields (Table 2) until a significant drop in activity was observed, which was accompanied by an intense yellow coloration of the solution.

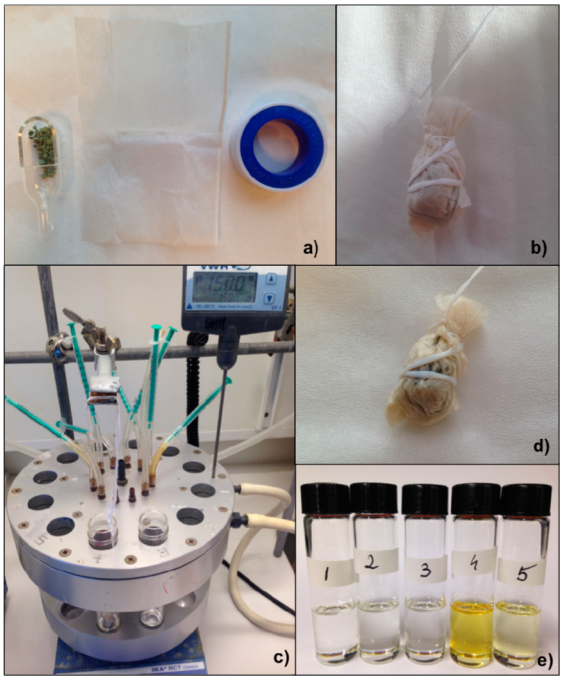

Figure 4. (a) Ingredients for the preparation of the catalytic teabag, (b) catalytic teabag before use, (c) reaction setup using a Radley carousel for reactions open to air, (d) catalytic teabag after five runs, and (e) change in color upon deactivation of the catalyst.

Table 2. Conversion and Metallic Leaching over Five Runs during the Catalyst Recycling Experiment in the Oxidation of 1a

run	conversion (%)	Pd leaching (ppm)	Cr leaching (ppm)
1	85	0.2	0.3
2	86	0.1	0.3
3	82	0.8	0.3
4	71	11.1	0.8
5	38	0.8	0.4

Although the teabag approach led to a convenient handling of the material, its rather rapid deactivation under these conditions was not satisfactory. One of the main limitations of the reaction under the conditions described above is the low solubility of air in BTX solvents (benzene, toluene, and xylene). This limitation was aggravated by the fact that stirring was significantly impeded, and no additional air-bubbling device was used.

AEROBIC OXIDATION UNDER CONTINUOUS FLOW

We predicted that a better mixing of the liquid and gaseous phases would drastically improve the reaction rate and would allow us to decrease the reaction temperature and prolong the lifetime of the catalyst. This hypothesis was implemented and evaluated in a continuous-flow setup, which led to an exceptional improvement over the reaction outcome.

1-Phenylethanol (**1a**) was chosen as a model substrate for oxidation in a continuous-flow regime, and synthetic air (20.9 ± 1% pure O_2) was used as the oxidizing agent. The instrumental setup was adapted for a three-phase reaction at high temperature, as schematically represented in Figure 5 (detailed procedure in Supporting Information). One of the essential components in the system is a microchip mixing device (1 mL volume, 1.6 m length microchannel) where the liquid phase (0.1 M, 1-phenylethanol in toluene) and gaseous phase (synthetic air) were pumped simultaneously (Movie S2). By precisely regulating the flow rates of the two components, very effective mixing is achieved before the reaction mass reaches the catalyst. This was decisive in order to achieve a satisfactory conversion in one pass through the reactor at only 110 °C, compared to 150 °C under batch conditions (vide supra).

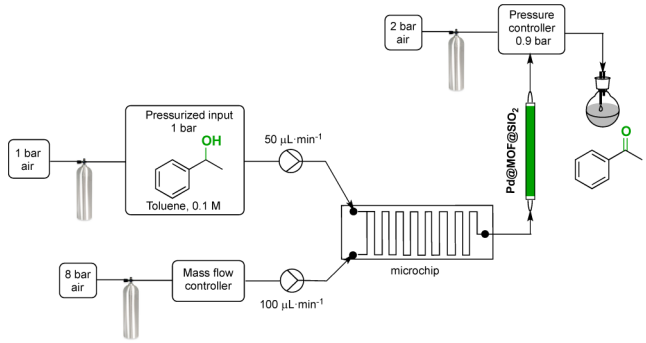

Figure 5. Instrumental setup for aerobic oxidation under continuous flow.

The packed-bed reactor consisted of a fritted-glass chromatography column loaded with 0.51 wt % Pd(0)@MIL-88B-NH_2@nano-SiO_2 (800 mg, 0.0385 mmol of Pd, ca. 40 mm bed height) and kept at a constant temperature of 110 °C. To avoid toluene evaporation, the reactor outlet was connected to a supplementary pressure controller that provided a back pressure of 0.9 bar. From the pressure controller, the reaction mixture was directed further to a collection flask. The residence time was determined to be ca. 10 min. Samples were collected regularly and analyzed by achiral gas chromatography to determine the conversion and by ICP-OES to measure the level of leached metallic species.

Initially, toluene was passed through the column for several minutes until the pressure was stabilized, followed by a mixture

dx.doi.org/10.1021/cs501573c | ACS Catal. 2015, 5, 472−479

toluene/MeOH (100:1) (details in Supporting Information, Section S1.5). It was found that this treatment inhibits the formation of acetals as byproducts, presumably by methanol coordination to the free Lewis acid sites of the chromium clusters.[35] Subsequently, the column was washed again with toluene and the reaction mixture was pumped in the microchip where it was intensively mixed with air, and the experiment was allowed to run continuously at 150 μL/min (50 μL/min and 100 μL/min for liquid and gaseous phases, respectively) for 1 week during which the catalyst displayed surprisingly stable behavior. The conversion stabilized after the first 6 h and remained almost constant at around 80% (~75% acetophenone + ~5% ethylbenzene) until the experiment was stopped after 7 days (168 h). The evolution of the yields of acetophenone and ethylbenzene in time is plotted in Figure 6 (all data points in Supporting Information, Table S5).

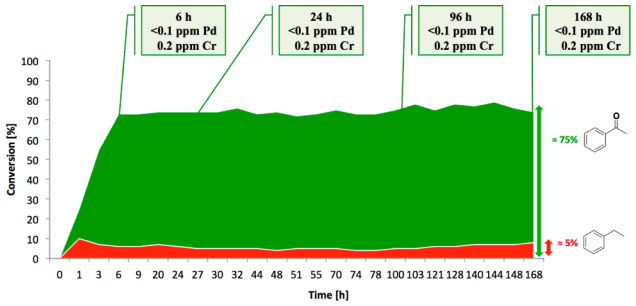

Figure 6. Conversion and metallic leaching in the aerobic oxidation of 1-phenylethanol catalyzed by 0.51 wt % Pd(0)@MIL-88B-NH_2@SiO_2 over 7 days.

The product was collected between 6 and 168 h and isolated by distillation from toluene using a Vigreux column, followed by column chromatography to yield 31.02 mmol (3.722 g) of isolated acetophenone corresponding to a TOF of 4.97 h^{-1}. Most importantly, throughout the whole experiment (samples measured at 6, 24, 96, and 168 h) the level of leached palladium remained below the detection limit of the ICP-OES technique (<0.1 ppm), whereas the chromium levels in solution were constant at 0.2 ppm.

The recovered catalyst was washed with toluene and twice with ethanol and then characterized. The XRPD pattern showed that the recycled Pd@MIL-88B-NH_2@nano-SiO_2 material remained crystalline (ESI, Figure S4). The ICP-OES analysis revealed a limited degradation of the framework. The C, H, and N contents were slightly lower in the recycled material whereas the content of metallic species increased from 0.51 to 0.62 wt % for palladium and from 0.96 to 1.22 wt % for chromium (ESI, Table S6). This result suggests that the silica matrix is very efficient at retaining the metallic species and preventing the contamination of the final product, even upon MOF degradation. This special property of the silica is also confirmed by the TEM images of the recycled material, which show a tendency of Pd to agglomerate at the interface between the MOF and the SiO_2 particles (ESI, Figure S9).

The activation period observed during the experiments in a continuous-flow regime may be explained by an incomplete reduction of Pd(II) complexes upon treatment with $NaBH_4$. This was further supported by running a control experiment performed under anaerobic conditions. A conversion of 7% 1-phenylethanol to acetophenone was measured after running the reaction for 16 h at 150 °C under an inert argon atmosphere, where only the Pd(II) species can act as an oxidant. The limitations of $NaBH_4$ as a reducing agent for the synthesis of Pd nanoparticles supported on MOFs were recently highlighted in the literature,[36] and a detailed investigation of this scenario is currently underway in our laboratories.

CONCLUSIONS

We have developed a double-supported nanopalladium catalyst and reported the first successful immobilization of catalytically active metallic nanoparticles in the pores of the flexible and robust MIL-88B-NH_2 framework. The resulting Pd@MOF material is coated with a customized protective layer of mesoporous silica through an innovative approach that drastically increases the durability and recyclability of the catalyst.

Pd(0)@MIL-88B-NH_2@nano-SiO_2 can catalyze the aerobic oxidation of benzylic alcohols with very good efficiency while completely avoiding the formation of byproducts by simply performing the reaction in tubes open to air, avoiding the hazardous yet common bubbling of oxygen in a reaction mixture containing Pd and refluxing organic solvents. Importantly, no additional oxidants or additives were required. Pd(0)@MIL-88B-NH_2@nano-SiO_2 was also used to prepare a catalytic teabag, which allowed us to recycle and reuse the catalyst in an extremely simple procedure that would be very easily scaled up. Even though the catalyst was deactivated fairly quickly when reused for five batches at 150 °C, the catalytic teabag method is extremely efficient at recovering all of the catalyst from the reaction mixture with minimal leaching of metallic species and is a promising solution for large-scale processes.

By adapting the reaction to a continuous-flow process in which a much better mixing of air and starting materials was achieved, we were able to decrease the temperature to 110 °C while maintaining the same performance of the catalyst. Under these conditions, Pd(0)@MIL-88B-NH_2@nano-SiO_2 could be used for at least 7 days, showing no signs of deactivation in continuous operation at a turnover frequency of 5 h^{-1}.

The extraordinary stability of Pd(0)@MIL-88B-NH_2@nano-SiO_2 under these conditions represents conclusive proof that the deposition of the MOF in the silica matrix has a tremendous beneficial effect on the framework. The protective properties of the SiO_2 coating together with the adaptation of the catalytic system to operation under continuous flow lead to a radical improvement in the methodology for the aerobic oxidation of benzylic alcohols. This reaction was redesigned as a safer and cleaner process, which could be more attractive for scale up.

ASSOCIATED CONTENT

Supporting Information

The following files are available free of charge on the ACS Publications website at DOI: 10.1021/cs501573c.

Further experimental details and spectroscopic measurements and analysis (PDF)

Movie S1; Beneficial effect of the innovative silica protective layer over the recyclability of the new material demonstrated in a teabag experiment (MPG)

Movie S2; Microchip mixing device in which the liquid phase and gaseous phase are pumped simultaneously (MPG)

dx.doi.org/10.1021/cs501573c | ACS Catal. 2015, 5, 472−479

AUTHOR INFORMATION

Corresponding Authors

*E-mail: xzou@mmk.su.se.
*E-mail: belen@organ.su.se

Author Contributions

#V.P. and A.B.G. contributed equally.

Notes

The authors declare no competing financial interest.
Inquiries related to the work on continuous flow should be addressed to mapericas@iciq.es.

ACKNOWLEDGMENTS

This project was supported by the Swedish Governmental Agency for Innovation Systems (VINNOVA) and AstraZeneca through the Berzelii Center EXSELENT, by the Swedish Research Council (VR) through project grants to B.M.-M and X.Z. and the MATsynCELL project through the Röntgen Ångström Cluster, and by the Knut and Alice Wallenberg Foundation (Catalysis in Selective Organic Synthesis and 3DEM-NATUR). The work on flow chemistry was funded by MINECO (grant CTQ2012-38594-C02-01), DEC (grant 2009SGR623), and the ICIQ Foundation. ICIQ authors also thank EU-ITN network Mag(net)icFun (PITN-GA-2012-290248) for financial support. B.M.-M. was supported by VINNOVA through a VINNMER grant. V.P. is grateful to the EU-ITN network Mag(net)icFun (PITN-GA-2012-290248) for appointment at ICIQ. C.A. thanks MICINN for a Juan de la Cierva postdoctoral fellowship.

REFERENCES

(1) Davis, S. E.; Ide, M. S.; Davis, R. J. *Green Chem.* **2013**, *15*, 17−45.
(2) For a review on the scope and limitations of oxidation reactions using O_2 as oxidant, see Shi, Z.; Zhang, C.; Tanga, C.; Jiao, N. *Chem. Soc. Rev.* **2012**, *41*, 3381−3430.
(3) For a comprehensive and comparative review on aerobic oxidation of alcohols catalyzed by various transition metals, see Parmeggiani, C.; Cardona, F. *Green Chem.* **2012**, *14*, 547−564.
(4) Arends, I. W. C. E.; Sheldon, R. A. *Appl. Catal., A* **2001**, *212*, 175−187.
(5) (a) Shokouhim, M.; Shin, K.-Y.; Lee, J. S.; Hackett, M. J.; Jun, S. W.; Oh, M. H.; Jang, J.; Hyeon, T. *J. Mater. Chem.* **2014**, *2*, 7593−7599. (b) Karami, K.; Ghasemi, M.; Haghighat Naeini, N. *Catal. Commun.* **2013**, *38*, 10−15. (c) Johnston, E. V.; Verho, O.; Kärkäs, M. D.; Shakeri, M.; Tai, C.-W.; Palmgren, P.; Eriksson, K.; Oscarsson, S.; Bäckvall, J.-E. *Chem.—Eur. J.* **2012**, *18*, 12202−12206. (d) Wu, H.; Zhang, Q.; Wang, Y. *Adv. Synth. Catal.* **2005**, *10*, 1356−1360.
(6) Uozumi, Y.; Nakao, R. *Angew. Chem., Int. Ed.* **2003**, *42*, 194−197.
(7) Karimi, B.; Abedi, S.; Clark, J. H.; Budarin, V. *Angew. Chem., Int. Ed.* **2006**, *45*, 4776−4779.
(8) Enache, D. I.; Edwards, J. K.; Landon, P.; Solsona-Espriu, B.; Carley, A. F.; Herzing, A. A.; Watanabe, M.; Kiely, C. J.; Knight, D. W.; Hutchings, G. J. *Science* **2006**, *311*, 362−365.
(9) (a) *Metal-Organic Frameworks: Design and Application*; Eddaoudi, M., Eubank, J. F., MacGillivray, L. R., Eds.; John Wiley and Sons, 2010; p 37. (b) For a dedicated issue comprising 18 review articles covering MOF structures, applications, synthesis, and properties, see *Chem. Rev.* **2012**, *112*, 673−674.
(10) (a) For a concise description of the fundamental principles of catalysis with MOFs, see Ranocchiari, M.; van Bokhoven, J. A. *Phys. Chem. Chem. Phys.* **2011**, *13*, 6388−6396. (b) For a comparative review on MOF and zeolite catalysts, see, Dhakshinamoorthy, A.; Alvaro, M.; Corma, A.; Garcia, H. *Dalton Trans.* **2011**, *40*, 6344−6360. (c) For a comprehensive manual on all aspects of MOFs synthesis, characterization, and applications in catalysis, see *Metal Organic Frameworks as Heterogeneous Catalysts*; Llabrés i Xamena, F. X., Gascon, J., Eds.; RSC Publishing: Cambridge, U.K., 2013; pp 237−424.
(11) (a) Gustafsson, M.; Bartoszewicz, A.; Martín-Matute, B.; Sun, J.; Grins, J.; Zhao, T.; Li, Z.; Zhu, G.; Zou, X. *Chem. Mater.* **2010**, *22*, 3316−3322. (b) Carson, F.; Agrawal, S.; Gustafsson, M.; Bartoszewicz, A.; Moraga, F.; Zou, X.; Martín-Matute, B. *Chem.—Eur. J.* **2012**, *18*, 15337−15334. (c) Platero-Prats, A. E.; Bermejo Gómez, A.; Samain, L.; Zou, X.; Martín-Matute, B. *Chem.—Eur. J.* **2014**, DOI: 10.1002/chem.201403909. (d) Pascanu, V.; Hansen, P.; Bermejo Gómez, A.; Ayats, C.; Platero-Prats, A. E.; Johansson, M. J.; Pericàs, M. À.; Martín-Matute, B. *ChemSusChem* **2014**, *7*, DOI 10.1002/cssc.201402858. For a related article, see (e) Tao Yang, T.; Bartoszewicz, A.; Ju, J.; Sun, J.; Liu, Z.; Zou, X.; Wang, Y.; Li, G.; Liao, F.; Martín-Matute, B.; Lin, J. *Angew. Chem., Int. Ed.* **2011**, *50*, 12555−12558.
(12) (a) (Review) Tanabe, K. K.; Cohen, S. M. *Chem. Soc. Rev.* **2011**, *40*, 498−519. (b) Song, Y.-F.; Cronin, L. *Angew. Chem., Int. Ed.* **2008**, *47*, 4635−4637. (c) Savonnet, M.; Cockrick, E.; Camarata, A.; Bazer-Bachi, D.; Bats, N.; Lecocq, V.; Pinel, C.; Farrusseng, D. *New J. Chem.* **2011**, *35*, 1892−1897.
(13) (a) (Review) Dhakshinamoorthy, A.; Garcia, H. *Chem. Soc. Rev.* **2012**, *41*, 5262−5284. (b) Zhu, Q.-L.; Li, J.; Xu, Q. *J. Am. Chem. Soc.* **2013**, *135*, 10210−10213. (c) Zahmakiran, M. *Dalton Trans.* **2012**, *41*, 12690−12696. (d) Jiang, H.-L.; Akita, T.; Ishida, T.; Haruta, M.; Xu, Q. *J. Am. Chem. Soc.* **2011**, *133*, 1304−1306.
(14) Chen, G.; Wu, S.; Liu, H.; Jiang, H.; Li, Y. *Green Chem.* **2013**, *15*, 230−235.
(15) Fei, H.; Shin, J.; Meng, Y. S.; Adelhardt, M.; Sutter, J.; Meyer, K.; Cohen, S. M. *J. Am. Chem. Soc.* **2014**, *136*, 4965−4973.
(16) Abedi, S.; Morsali, A. *ACS Catal.* **2014**, *4*, 1398−1403.
(17) Tan, J. C.; Cheetham, A. K. *Chem. Soc. Rev.* **2011**, *40*, 1059−1080.
(18) Li, Z.; Zheng, H. C. *J. Am. Chem. Soc.* **2014**, *136*, 5631−5639.
(19) (a) Pascanu, V.; Yao, Q.; Bermejo Gómez, A.; Gustafsson, M.; Yun, Y.; Wan, W.; Samain, L.; Zou, X.; Martín-Matute, B. *Chem.—Eur. J.* **2013**, *19*, 17483−17493. (b) Pan, Y.; Yuan, B.; Li, Y.; He, D. *Chem. Commun.* **2010**, *46*, 2280−2282. (c) Yuan, B.; Pan, Y.; Li, Y.; Yin, B.; Jiang, H. *Angew. Chem., Int. Ed.* **2010**, *24*, 4054−4058.
(20) (a) Chen, L.; Chen, H.; Luque, R.; Li, Y. *Chem. Sci.* **2014**, *5*, 3708−3714. (b) Zhang, D.; Guan, Y.; Hensen, E.; Xue, T.; Wang, Y. *Catal. Sci. Technol.* **2014**, *4*, 795−802. (c) Huang, Y.; Zheng, Z.; Liu, T.; Lü, J.; Lin, Z.; Li, H.; Cao, R. *Catal. Commun.* **2011**, *14*, 27−31.
(21) Bernt, S.; Guillerm, V.; Serre, C.; Stock, N. *Chem. Commun.* **2011**, *47*, 2838−2840.
(22) (a) Poliakoff, M.; Fitzpatrick, J. M.; Farren, T. R.; Anastas, P. T. *Science* **2002**, *297*, 807−810. (b) Collins, T. *Science* **2001**, *291*, 48−49.
(23) (Review) Anastas, P.; Eghbali, N. *Chem. Soc. Rev.* **2010**, *39*, 301−312.
(24) (a) Russell, D. A. M.; Shiang, D. L. *ACS Sustainable Chem. Eng.* **2013**, *1*, 2−7. (b) Hansen, K. B.; Hsiao, Y.; Xu, F.; Rivera, N.; Clausen, A.; Kubryk, M.; Krska, S.; Rosner, T.; Simmons, B.; Balsells, J.; Ikemoto, N.; Sun, Y.; Spindler, F.; Malan, C.; Grabowski, E. J. J.; Armstrong, J. D., III. *J. Am. Chem. Soc.* **2009**, *131*, 8798−8804. (c) Calvo-Flores, F. G. *ChemSusChem* **2009**, *2*, 905−919. (d) Sheldon, R. A. *Green Chem.* **2008**, *10*, 359−360. (e) Horvath, I.; Anastas, P. *Chem. Rev.* **2007**, *107*, 2169−2173.
(25) Office of Pollution Prevention and Toxics, The Presidential Green Chemistry Challenge Awards Program, Summary of 2008 Award Entries and Recipients, U.S. Environmental Protection Agency: Washington DC, EPA 744R08002, 2008.
(26) Shih, Y.-H.; Lo, S.-H.; Yang, N. S.; Singco, B.; Cheng, Y.-J.; Wu, C.-Y.; Chang, I.-H.; Huang, H.-Y.; Lin, C.-H. *ChemPlusChem.* **2012**, *77*, 982−986.
(27) Nondry methanol was used as the solvent for the impregnation of Pd(II) in MIL-88B-NH_2.
(28) Serre, C.; Mellot-Draznieks, C.; Surblé, S.; Audebrand, N.; Filinchuk, Y.; Feréy, G. *Science* **2007**, *315*, 1828−1831.
(29) Elemental analysis: Found: Cr, 14.15; Pd, 7.40. Calculated: Cr, 15.45; Pd, 7.38. Based on $[Cr_3O(O_2C\text{-}C_6H_3NH_2\text{-}CO_2)_3F(H_2O)_2(PdCl_2)_{0.7}\cdot CH_3CN\cdot 4H_2O]$.

(30) No peaks corresponding to crystalline palladium could be observed in the diffraction pattern.
(31) Search on the Cambridge Crystallographic Database over 1372 reported crystal structures of palladium complexes with the proposed coordination environment $[Pd(II)(ArNH_2)_2Cl_2]$ gave average values of Pd−N = 2.03(6) Å and Pd−Cl = 2.30(2) Å.
(32) Horcajada, P.; Salles, F.; Wuttke, S.; Devic, T.; Heurtaux, D.; Maurin, G.; Vimont, A.; Daturi, M.; David, O.; Magnier, E.; Stock, N.; Filinchuk, Y.; Popov, D.; Riekel, C.; Férey, G.; Serre, C. *J. Am. Chem. Soc.* **2011**, *133*, 17839−17847.
(33) Carson, F.; Su, J.; Platero-Prats, A. E.; Wan, W.; Yun, Y.; Samain, L.; Zou, X. *Cryst. Growth Des.* **2013**, *13*, 5036−5044.
(34) Sing, K. S. W.; Everett, D. H.; Haul, R. A. W.; Moscou, L.; Pierotti, R. A.; Rouquerol, J.; Siemieniewska, T. *Pure Appl. Chem.* **1985**, *57*, 603−619.
(35) When methanol was used as a cosolvent (10% v/v) throughout the whole experiment, a quick deactivation of the catalyst was observed within the first 4 to 5 h.
(36) Zhang, D.; Guan, Y.; Hensen, E. J. M.; Xue, T.; Wang, Y. *Catal. Sci. Technol.* **2014**, *4*, 795−802.